Climate Dynamics (2005)
DOI 10.1007/s00382-005-0021-8

Haijun Yang · Zhengyu Liu

# Tropical–extratropical climate interaction as revealed in idealized coupled climate model experiments

Revised: 3 February 2005 / Accepted: 4 March 2005


**Abstract** Tropical–extratropical climate interactions are studied by idealized experiments with a prescribed 2°C SST anomaly at different latitude bands in a coupled climate model. Instead of focusing on intrinsic climate variability, this work investigates the mean climate adjustment to remote external forcing. The extratropical impact on tropical climate can be as strong as the tropical impact on extratropical climate, with the remote sea surface temperature (SST) response being about half the magnitude of the imposed SST change in the forcing region. The equatorward impact of extratropical climate is accomplished by both the atmospheric bridge and the oceanic tunnel. About two-thirds of the tropical SST change comes from the atmospheric bridge, while the remaining one-third comes from the oceanic tunnel. The equatorial SST increase is first driven by the reduced latent heat flux and the weakened poleward surface Ekman transport, and then enhanced by the decrease in subtropical cells' strength and the equatorward subduction of warm anomalies. In contrast, the poleward impact of tropical climate is accomplished mainly by the atmospheric bridge, which is responsible for extratropical temperature changes in both the surface and subsurface. Sensitivity experiments also show the dominant role of the Southern Hemisphere oceans in the tropical climate change.

CCR contribution number 829; DAS-PKU contribution number 002.

H. Yang (✉)
Department of Atmospheric Science and Laboratory for Severe Storm and Flood Disasters, School of Physics, Peking University, 209 Chengfu Road, Beijing, China100871,
E-mail: hjyang@pku.edu.cn

Z. Liu
Center for Climatic Research and Department of the Atmospheric and Oceanic Sciences, University of Wisconsin-Madison, Madison, WI USA

## 1 Introduction

It has been established that the tropical climate change has a significant impact on the global climate through the atmospheric bridge (e.g., Lau 1997; Schneider et al. 1997; Alexander et al. 2002). Observational and modeling studies have demonstrated a clear link between sea surface temperature (SST) anomalies in the equatorial Pacific with those in the North Pacific (Zhang and Wallace 1996; Lau 1997; Zhang et al. 1998a; Wang 2002), north tropical Atlantic (Enfield and Mayer 1997), North Atlantic (Hoerling et al. 2001; Lu et al. 2004) and Indian Oceans (Yu and Rienecker 1999) on interannual to interdecadal timescales. The tropical ocean changes alter the surface air temperature, humidity, wind, as well as the cloud distribution, which eventually induce changes in climate of remote regions through the quasistationary planetary wave or storm tracks (Lau 1997; Alexander et al. 2002). For example, recent studies have suggested that the North Atlantic climate change might originate from the tropical Indian and Pacific Oceans (Hoerling et al. 2001) or tropical eastern Pacific (Lu et al. 2004). The widespread continental droughts in the United States, southern Europe and Southwest Asia during 1998–2002 could also link to the persistent tropical ocean SST anomalies during the same period (Hoerling and Kumar 2003).

The extratropical climate, however, can also affect the tropics through both the atmospheric bridge and oceanic tunnel (Gu and Philander 1997; Kleeman et al. 1999; Barnett et al. 1999; Pierce et al. 2000), generating interdecadal and long-term climate changes. Unlike the tropical impacts on the extratropics, the oceanic processes are involved in the extratropical-driven tropical low frequency variability. The anomalous signals in subtropical ventilation zone can be transported equatorward by mean subduction flow and disturb the tropical climate. The changes in the strength of meridional overturning circulation can also cause the tropical

temperature to change by varying the amount of equatorward cold-water transport (Kleeman et al. 1999; Nonaka et al. 2002).

A recent work by Liu and Yang (2003) (LY03, hereafter) provides a quantitative assessment of the tropical–extratropical mean climate interaction in a fully coupled climate system. LY03 shows that the oceanic dynamics accounts for one-third of the total equatorial surface temperature change. The extratropics plays the same important role as the tropics does in the global climate change, especially on interdecadal or longer timescales. However, there are still several questions remaining to be clarified. For instance, the model experiments were not described in details. And it was not made clear how the tropical air-sea system responds to the changes in Hadley cells and meridional overturning circulations. The concrete physical processes that are responsible for the tropical SST change need to be pinpointed.

This work complements LY03 and provides more detailed analyses on the mechanisms of the extratropical–tropical climate interaction. In addition, we further examine the relative roles of the Northern Hemisphere (NH) and Southern Hemisphere (SH) in the tropical climate change as well as the interhemispheric climate interaction. This paper systematically rechecks the problem of LY03 and is an attempt to provide a panorama of the climate interaction among different regions through both the atmospheric bridge and oceanic tunnel. As mentioned in LY03, this paper, instead of focusing on intrinsic climate variabilities, investigates the mean climate response in one region to a remote climate disturbance in another.

Using a so-called ''partial coupling'' (PC) technique in a fully coupled climate model, sensitivity experiments are performed to quantify the mean climate change in a remote region and the relative roles of atmospheric bridge and oceanic tunnel in the tropical–extratropical interactions, and further, to reveal the mechanisms of these interactions. It is found that the extratropical impact on the tropics could be as strong as the tropical impact on extratropical climate. The initially rapid SST change in the remote region is usually caused by the rapid Hadley cell adjustment. In contrast, the slow SST change in the remote region results from the change of subtropical cells' strength and the subduction of anomalous signals. A warm SST in the extratropics could force a tropical SST warming of about half its magnitude, in which about two-thirds of the SST change comes from the atmospheric bridge, while the remaining one-third comes from the oceanic tunnel. A warm SST in the tropics could also force an extratropical surface and subsurface warming of about half its magnitude, which is, however, accomplished predominantly by the atmospheric bridge. The SH contributes more than the NH to the equatorial temperature change due to the hemispheric asymmetry of the Hadley cell. In addition, the SH SST warming can cause significant remote climate change in the NH and vice versa. The NH climate response to the SH forcing could be faster and stronger than the SH climate response to the NH forcing. This study, to some extent, appears to emphasize the dominant role of the SH in the global climate change.

This work can be understood as relevant to the problem of mechanisms of climate adjustment to slow external forcing. The prescribed 2°C SST warming in extratropics or tropics in the sensitivity experiments is well beyond the range of intrinsic coupled variability, but is within the range of the SST change for a doubling of $CO_2$ (Kerr 2004; Lea 2004). This strong anomalous signal is necessary in order to generate significant change in the remote region. All the results obtained here are appropriate for our model but could be model-dependent. We expect that the physical processes examined here and our understanding of climate adjustment to external forcing could be helpful to understand reality.

This paper is arranged as follows. Section 2 introduces the coupled model and PC experiments. Section 3 studies the extratropical impact on the tropical climate and associated changes in various climate quantities such as equatorial SST and thermocline, the atmospheric Hadley cells and oceanic overturning circulations. Section 4 investigates the tropical impact on the extratropical climate. Section 5 compares the hemispheric contribution to the equator and the interhemispheric interaction. Conclusions and discussions are provided in section 6.

## 2 The model and approach

The model used here is the fast ocean–atmosphere model (FOAM) developed jointly at University of Wisconsin-Madison and the Argonne National Laboratory (Jacob 1997). The Atmospheric model is a parallel version of the National Center for Atmospheric Research (NCAR) Community Climate Model version 2 (CCM2) but with the atmospheric physics replaced by those of CCM3. The ocean model was developed following the Geophysical Fluid Dynamics Laboratory (GFDL) Modular Ocean Model (MOM). The FOAM used here has an atmospheric resolution of R15 with 18 vertical layers in a hybrid sigma-pressure coordinate system and an oceanic resolution of 1.4° latitude×2.8° longitude×32 vertical levels. Without flux adjustment, the fully coupled control simulation (CTRL) has been integrated for over 1,000 years, showing no apparent climate drifts.

FOAM captures most major features of the observed climate. It has also been used successfully for the study of ENSO (Liu et al. 2000), Atlantic climate variability (Liu and Wu 2000) and Pacific decadal variability (Liu et al. 2002a; Wu et al. 2003). For example, the leading EOF of the anomalous model SST within the interannual band ($< 8$ year) is similar to the observed ENSO; the area-weighted pattern correlation between the model and observed EOFs is 0.82; the model ENSO has a realistic timescale and an amplitude of about 75% of the observed ENSO (Liu et al. 2000). The leading EOF of

decadal low-passed SST exhibits an ENSO-like pattern that also correlates well with observations (at 0.75) (Wu et al. 2003). The basic features of the simulated Pacific decadal variability have been seen in the observations (Barlow et al. 2001).

To quantify the dynamic impact of the climate change in one region on the climate in another remote region, "PC" technique is used in FOAM. Using this approach, full ocean–atmosphere coupling is allowed only in some selected region; elsewhere, the annual cycle of climatological SST from model CTRL is prescribed to force the model atmosphere or ocean. The PC provides an important modeling technique for assessing the individual role of the atmospheric bridge and oceanic tunnel in the interaction between different geographic regions (Wu et al. 2003; LY03).

Three experiments are performed to study the sensitivity of tropical (extratropical) climate to extratropical (tropical) forcing, which is taken as a 2°C SST warming. All the experiments start from the 800th year of the CTRL run and are integrated for 200 years, when the upper ocean has reached quasi-equilibrium. First, to assess the full impact of the extratropical forcing on tropical climate, a PC experiment ABOT (Atmospheric Bridge/Oceanic Tunnel) is performed, in which a 2°C SST anomaly is "seen" by both the atmosphere and ocean in the global extratropics ($>|30°|$ latitude) and is then "carried" equatorward by both the atmospheric bridge and oceanic tunnel (Fig. 1a). Specifically, the ocean and atmosphere in ABOT remain fully coupled within the global tropics ($<|30°|$ latitude), but become only partially coupled in the extratropics. There, the atmosphere is always forced by the heat flux that is calculated based on the prescribed SST seasonal cycle of the CTRL plus 2°C; while the ocean is forced by calculated atmospheric fluxes through the coupler. Second, a complementary experiment T-ABOT is performed to assess the impact of tropical forcing on the extratropical climate, in which the regions of full coupling and PC of ABOT are swapped such that the ocean and atmosphere remain fully coupled in the extratropics, but both "see" a 2°C SST warming in the global tropics (Fig. 1b). Third, to quantify the individual role of the atmospheric bridge and oceanic tunnel, an Oceanic Tunnel (OT) experiment is conducted. It is the same as ABOT except for a modified PC in the extratropics. There, the surface ocean is restored toward the prescribed SST seasonal cycle of CTRL plus 2°C, while the atmosphere is forced by the prescribed SST seasonal cycle of CTRL only (Fig. 1c). As such, only the ocean "sees" a 2°C SST

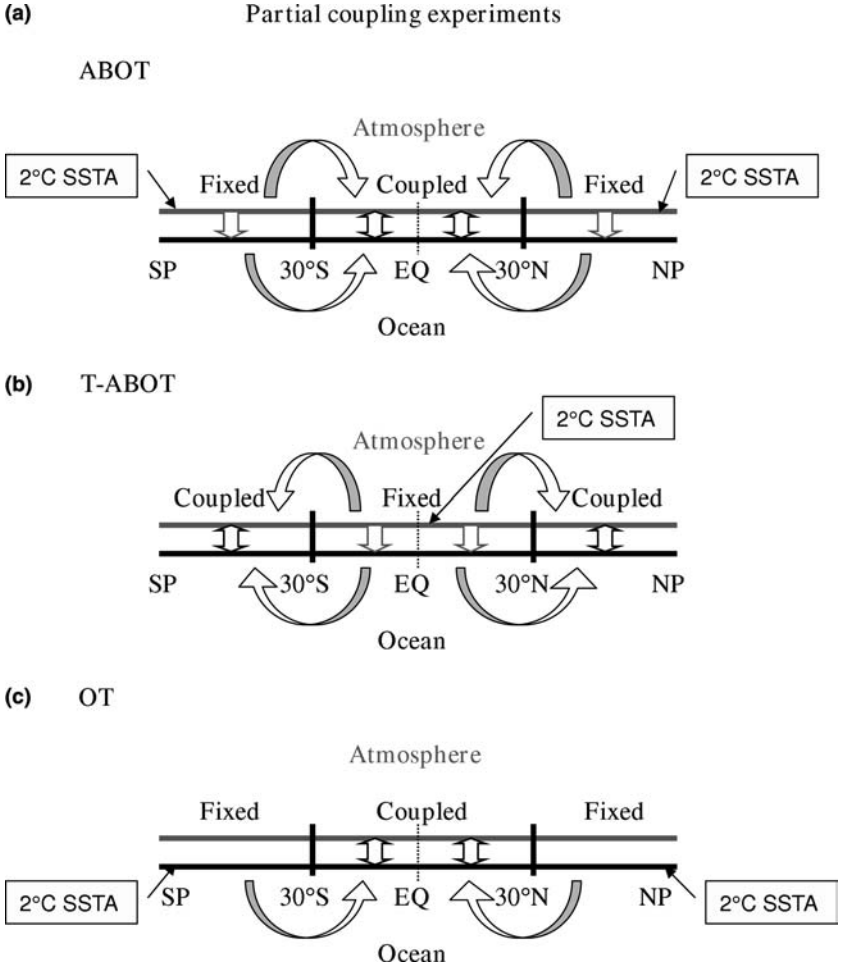


**Fig. 1** Schematic diagram of PC experiments **a** ABOT, **b** T-ABOT and **c** OT. In ABOT, both the atmosphere and ocean in the global extratropics ($>|30°|$ latitude) "see" a 2°C SST anomaly. In T-ABOT, the global tropical ocean and atmosphere ($<|30°|$ latitude) "see" a 2°C SST anomaly. In OT, only the extratropical ocean "sees" a 2°C SST anomaly

warming and therefore, contributes to the equatorward subduction of extratropical SST anomaly.

For each PC experiment, a parallel PC control simulation is performed. All the climate anomalies here are derived as the difference between each PC experiment and its respective control. Each PC control simulation is performed to avoid the model drift that may arise due to the PC scheme. Therefore, each PC control has exactly the same configuration as the PC sensitivity experiment except in the PC region where no anomalous SST is added to the prescribed seasonal cycle of CTRL (e.g., the extratropical SST to the atmosphere is prescribed simply as the seasonal cycle of CTRL for the control of ABOT). These PC controls do not have significant drifts from the fully coupled CTRL, such that our major results do not change significantly regardless of using the PC control or the fully coupled CTRL as the base run to derive climate anomalies.

## 3 Extratropical impact on tropical climate

### 3.1 Changes in equatorial SST and thermocline

A 2°C SST warming in the global extratropics can increase equatorial SST by about 1°C. Experiment ABOT shows that after the onset of the extratropical warming, equatorial SST increases rapidly by more than 0.5°C in the first few years, reflecting a quick extratropical impact through the atmospheric bridge, and reaches a quasi-equilibrium after several decades (Fig. 2a). The final SST warming is about 0.9°C. In comparison, subsurface temperature increases gradually, especially in the first 50 years (Fig. 2b). The final upper ocean temperature warms about the same as the SST (~1.0°C), reflecting a deep equatorial warming (Fig. 3b2). Therefore, a warming SST in the extratropics can force a tropical SST warming of about half its magnitude, representing a significant extratropical control on tropical climate.

The extratropical impact on the tropical climate in ABOT is accomplished by both the atmospheric bridge and OT. The individual effect of the atmospheric bridge and OT can be qualified with experiment OT. Figure 2a shows that in OT, the equatorial SST increases gradually, becoming statistically significant (at 99% level) after 20–30 years. The final equatorial SST warms about 0.26°C. This accounts for about 30% of the final SST warming in ABOT, implying a remaining 70% contribution from the atmosphere bridge. The equatorial subsurface temperature change in OT is comparable with that in ABOT (Fig. 2b). The relative contribution of the atmospheric (70%) and oceanic (30%) bridges is also confirmed by another sensitivity experiment that only has the atmospheric bridge (AB, not shown). In AB, the oceanic teleconnection tunnel is "blocked" by inserting a "sponge wall" at 27–33° latitude bands in which temperature and salinity are restored toward their seasonal climatology (Wu et al. 2003). The final SST

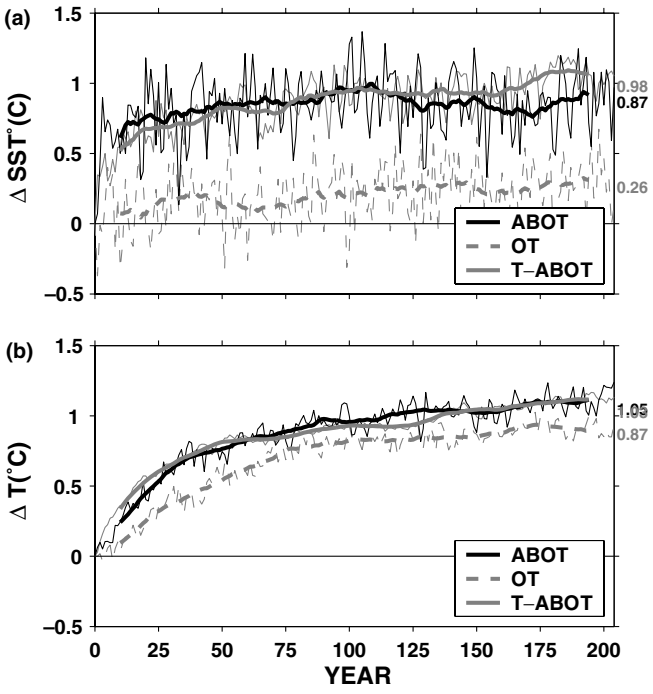


**Fig. 2** Evolution of anomalous annual mean **a** SST and **b** upper ocean temperature (40–400 m average) in ABOT (*solid black*), T-ABOT (*solid grey*) and OT (*dashed grey*). The temperature is averaged globally from 10°S to 10°N for ABOT and OT, and 30°N (S)–60°N (S) for T-ABOT. The 21-year running mean is also plotted for each curve as the heavy lines. The anomalous SST and subsurface temperature averaged in the last 100 years are labeled at the right edge of the figures. The anomaly in each experiment is relative to its own control run which has the identical settings as the respective PC experiments except for the absence of a 2°C SST anomaly on the prescribed seasonal cycle of CTRL

warming is about 0.6°C, accounting for about 70% of the total SST warming in ABOT.

The OT, while only contributing a small portion of the equatorial temperature change on the surface, dominates the change in the subsurface temperature. Indeed, over 80% of the subsurface temperature change in ABOT is accounted for by that in OT (Fig. 2b). The fast atmospheric bridge is ineffective in changing equatorial temperature in the subsurface because the strong equatorial upwelling inhibits the downward penetration of the effect of the surface atmospheric forcing.

In OT, the equatorial subsurface temperature change is due to the ocean subduction process. Figure 3d2 shows a pair of subsurface warm tongues penetrating equatorward (particularly clear from the south) and upward. The implied stronger oceanic contribution from the south is expected, because the northern influence is weakened by the ITCZ wind forcing (Lu et al. 1998) and Indonesia Throughflow (Rodgers et al. 1999). The final SST change generated by the ocean tunnel has a local maximum on the equator (Fig. 3d1). This maximum equatorial SST anomaly can also be observed in ABOT (Fig. 3b1), because of the role of the ocean tunnel there. In the equatorial upper ocean, the temperature anomaly

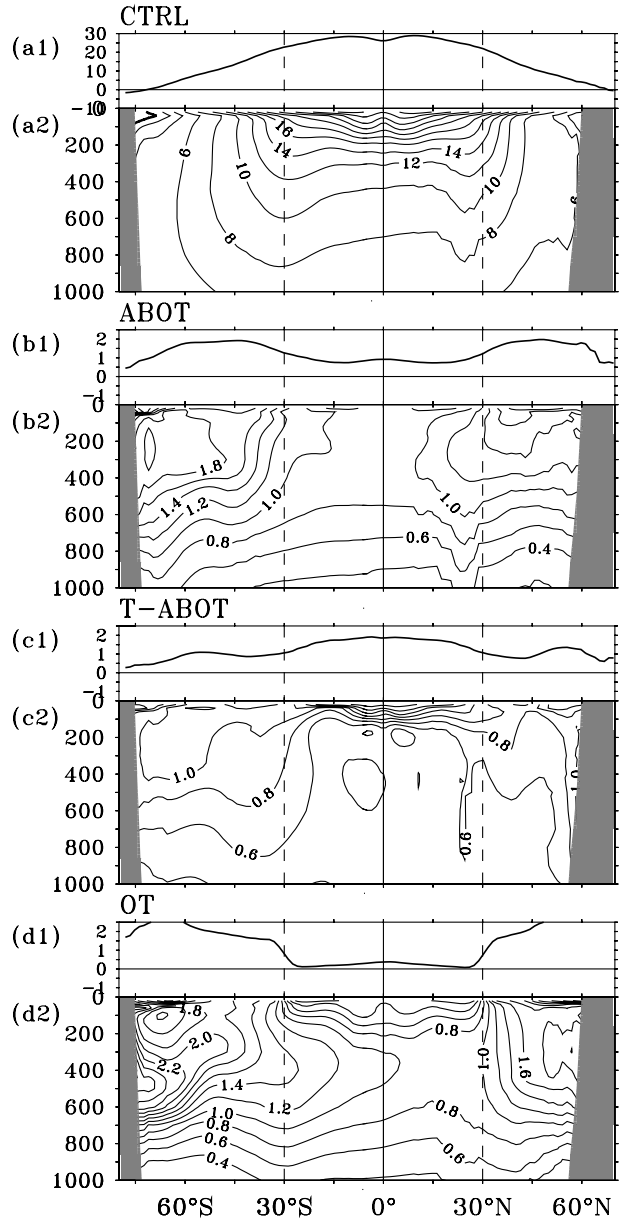


**Fig. 3** Zonal mean Pacific Ocean temperature averaged in year 150–200 for **b** ABOT, **c** T-ABOT and **d** OT. For reference, the mean temperature in CTRL is also plotted in (**a**). In each panel, the *upper figure* (a1, b1, c1 and d1) shows the **a** total or **b**–**d** anomalous zonal mean SST, while the *lower figure* (a2, b2, c2 and d2) shows the meridional section of zonal temperature change. Contour intervals for temperature are 2°C in (**a**) and 0.2°C in (**b**)–(**d**)

decreases upward toward the surface in OT (Fig. 3d2), but decreases downward toward the subsurface in ABOT (Fig. 3b2). This occurs because the SST is warmed from below by the ocean tunnel in OT, but mainly from above by the atmosphere bridge in ABOT.

The horizontal pattern shows an increased west–east SST contrast in the Pacific in both ABOT and OT (Fig. 4c, e). The maximum SST increase is located in the warm pool region, coinciding with the maximum zonal wind convergence ($\partial\tau'_x/\partial x$). The maximum trade wind decrease is located just to the west of the maximum SST increase. In ABOT the equatorial trade wind change is controlled by the Hadley cells, and is thus, insensitive to the change in equatorial zonal SST contrast. The enhanced zonal SST contrast in ABOT is consistent with the studies of simplified coupled model (Clement et al. 1996; Cane et al. 1997) and box models (Seager and Murtugudde 1997; Liu 1998). This model experiment, forced by a sudden spatially uniform warming in the extratropics, is qualitatively similar to the simplified coupled model experiments forced by a sudden spatially uniform heat flux heating in the tropics by Clement et al. (1996) and Cane et al. (1997). The warm pool is controlled by a thermodynamical feedback in which the SST must warm by as much as necessary for the upward surface heat flux to balance the imposed downward flux (Seager and Murtugudde 1997). The cold tongue is controlled by a dynamical feedback in which the cold-water upwelling retards the mean temperature increase (Cane et al. 1997). The "ocean dynamical thermostat" appears to be valid in our coupled GCM. This is unlike some coupled GCM simulations forced by greenhouse gas, in which the equatorial zonal SST contrast is reduced due to the cloud-albedo feedback (e.g., Meehl and Washington 1996; Timmermann et al. 1999).

The tropical thermocline temperature change averaged between 40–400 m shows more warming in the east in ABOT (Fig. 4d), but zonally uniform in OT (Fig. 4f). In ABOT, the oceanic overturning circulation is reduced in response to the weakened Hadley cells (we will show the details later). This requires a westward anomalous temperature gradient to geostrophically balance the poleward anomalous flow at depth (McPhaden and Zhang 2002). In OT, the overturning circulation is almost unchanged. The nearly zonally uniform anomalous temperature field (Fig. 4f) is consistent with zero anomalous meridional flow.

The general patterns in SST and thermocline in the idealized "regional warming" experiments may be different from the greenhouse gas forcing scenario and thus reality. However, instead of reproducing reality, the purpose in this work is to estimate the remote impact between different regions, and further to understand the mechanism of the climate adjustment to remote forcing, through these specially designed experiments.

### 3.2 Changes in Hadley cells and oceanic overturning circulation

The Hadley cell plays an important role in connecting the tropics with the extratropics. In ABOT, the final annual mean Hadley cell is weakened by more than 10%, with the change most visible in the SH (Fig. 5a), because the annual mean ITCZ is located north of the equator (Fig. 5b) and the sea surface area is larger in the SH. The weakened Hadley cell is a result of the reduced meridional SST gradient. As a result of the weakened Hadley cell, the annual mean equatorial trade wind is weakened by about 10% (Fig. 4c).

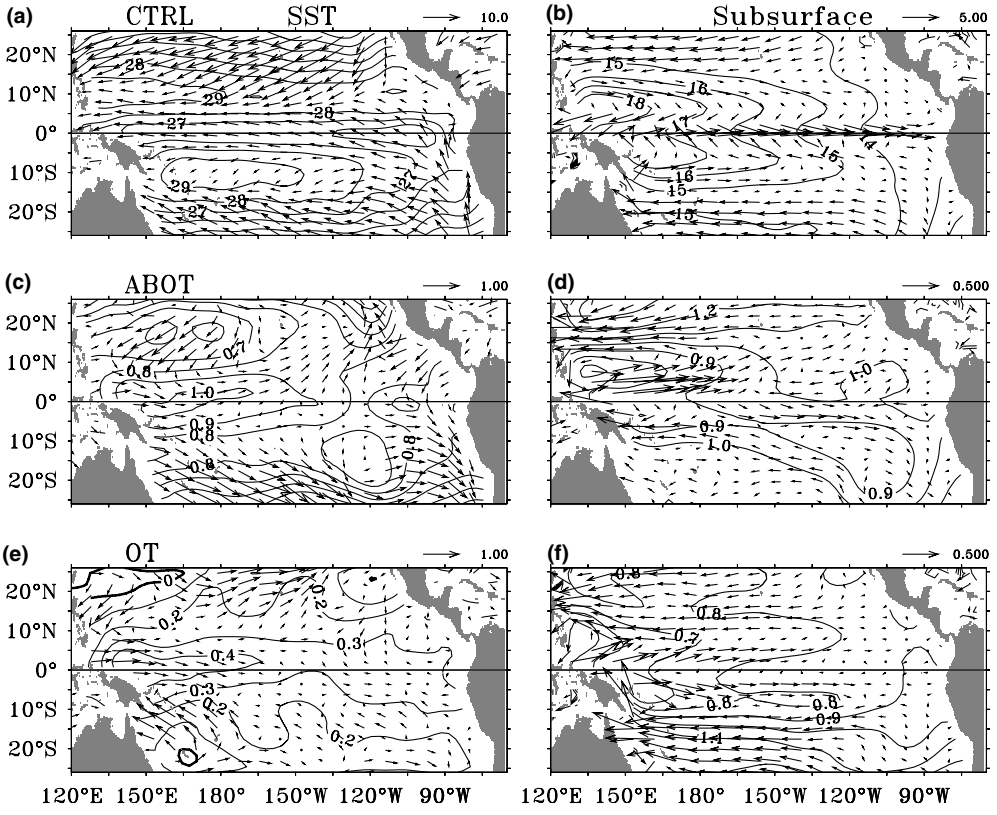


**Fig. 4** Anomalous Pacific Ocean (*left*) SST and wind stress, (*right*) subsurface temperature and current averaged between 40–400 m in year 150–200 for (**c**)–(**d**) ABOT and (**e**)–(**f**) OT. For reference, the mean SST–wind stress and subsurface temperature–current in CTRL are also plotted in (**a**) and (**b**), respectively. Contour intervals are 1°C in (**a**), (**b**) and 0.1°C for the rest. The reference vector of wind stress is $10\times10^{-2}$ N/m$^2$ in (**a**) and $1\times10^{-2}$ N/m$^2$ in (**c**) and (**e**). The reference vector for subsurface current is 5 cm/s in (**b**) and 0.5 cm/s in (**d**) and (**f**)

In ABOT the atmosphere in both hemispheres experiences remarkable changes. In boreal winter (December–January–February), the ascending branch of the Hadley cell is located at 15°S while the descending branch is located at 30°N (Fig. 5d). The change in Hadley cell is almost symmetric about the equator (Fig. 5c). The extratropical warming beyond 30°S induces a northward shift of the Hadley cell, because the sea surface area in the SH is much larger than that in the NH. This results in an anomalous ascending motion at 30–35°S. In boreal summer (June-July-August), the mean Hadley cell is opposite to that in winter, with the descending motion located at 30°S (Fig. 5f). The extratropical warming reduces the Hadley cell and causes anomalous ascending motion at 30–35° in both hemispheres (Fig. 5e). Again the Hadley cell changes the most in the SH because of larger sea surface area there.

The oceanic meridional overturning circulations in ABOT exhibit coherent changes with the Hadley cell changes because the strength of the former depends only on wind forcing (McCreary and Lu 1994). The annual mean meridional overturning circulations in the Pacific–the Subtropical Cells (STCs) (Fig. 6b) show that the subtropical water subducts in the region of downward Ekman pumping (around 30°N/S) and flows equatorward at depth, rises to the surface at the equator and returns poleward by means of Ekman drift under easterly winds (Liu et al. 1994). In ABOT, the annual mean STCs are weakened by over 10% (Fig. 6a) in response to the weakened Hadley cells (Fig. 5a). The southern STC is weakened more than the northern one because the southern Hadley cell is weakened more. In accordance with the mean Hadley cell patterns, the northern (southern) STC in boreal winter (summer) dominates the upper Pacific (Fig. 6d, f). Furthermore, consistent with the changes in Hadley cells, the most visible change in the northern (southern) STC in boreal winter (summer) occurs within 15° (30°) of the equator (Fig. 6c, e). At any time of the year, the local equatorial cells (the tight cells within about 5° of the equator in the upper 200 m) are also reduced significantly.

The change in STCs in this work, although obtained from an idealized experiment, is consistent with an observational study by McPhaden and Zhang (2002) in terms of dynamical mechanism. McPhaden and Zhang (2002) describe a slowdown of the Pacific shallow meridional overturning circulation (i.e., STC) from observations over the past 50 years. This slowdown of the STCs causes a decrease in upwelling of about 25% within 9° of the equator since 1970s, which is associated with a 0.8°C rise in equatorial SST. The slackening in STCs is a result of reduced equatorward Sverdrup transport in both hemispheres in the 1990s, which in turn is caused by the persistent westerly wind anomalies near the equator during the same period.

### 3.3 Changes in meridional heat transport

The meridional heat transport in the ocean–atmosphere system is closely related to atmospheric eddies' activities and the Hadley cells, as well as oceanic meridional

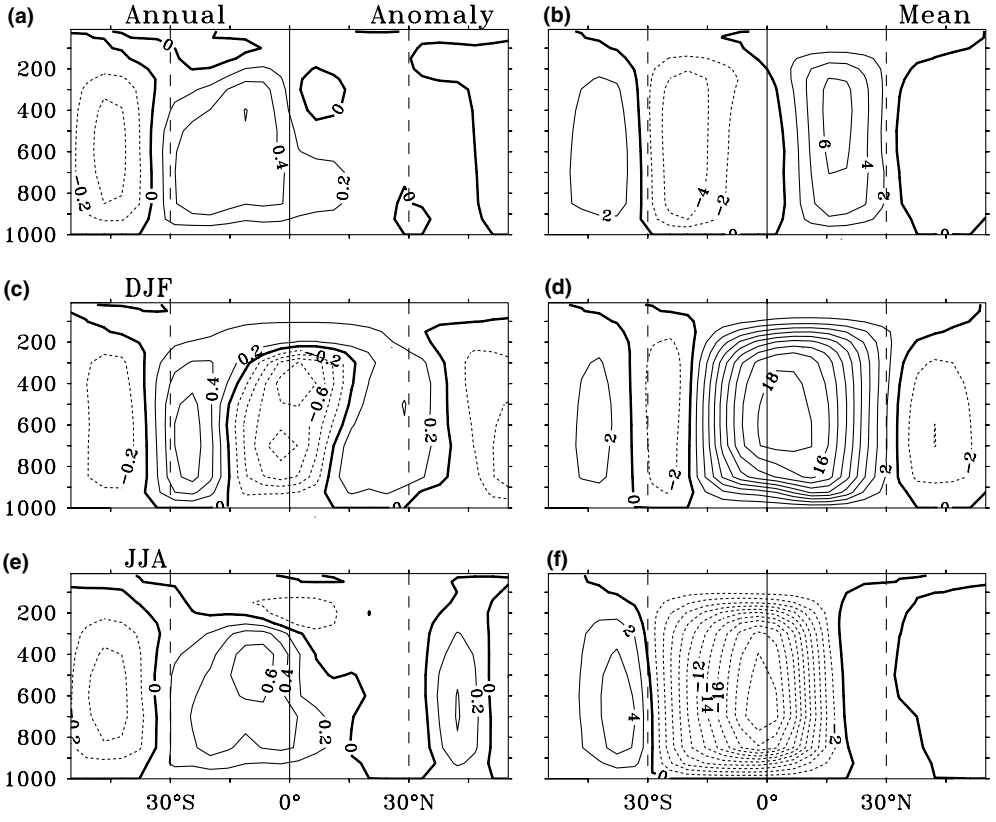


**Fig. 5** Meridional streamfunction of the global atmosphere for (*right column*) the CTRL and (*left column*) the difference between ABOT and its control averaged in year 150–200, for **a**, **b** annual mean, **c**, **d** DJF (December–January–February) and **e**, **f** JJA (June–July–August). Contour intervals are $0.2\times10^{10}$ Kg/s in (**a**), (**c**) and (**e**), and $2\times10^{10}$ Kg/s in (**b**), (**d**) and (**f**)

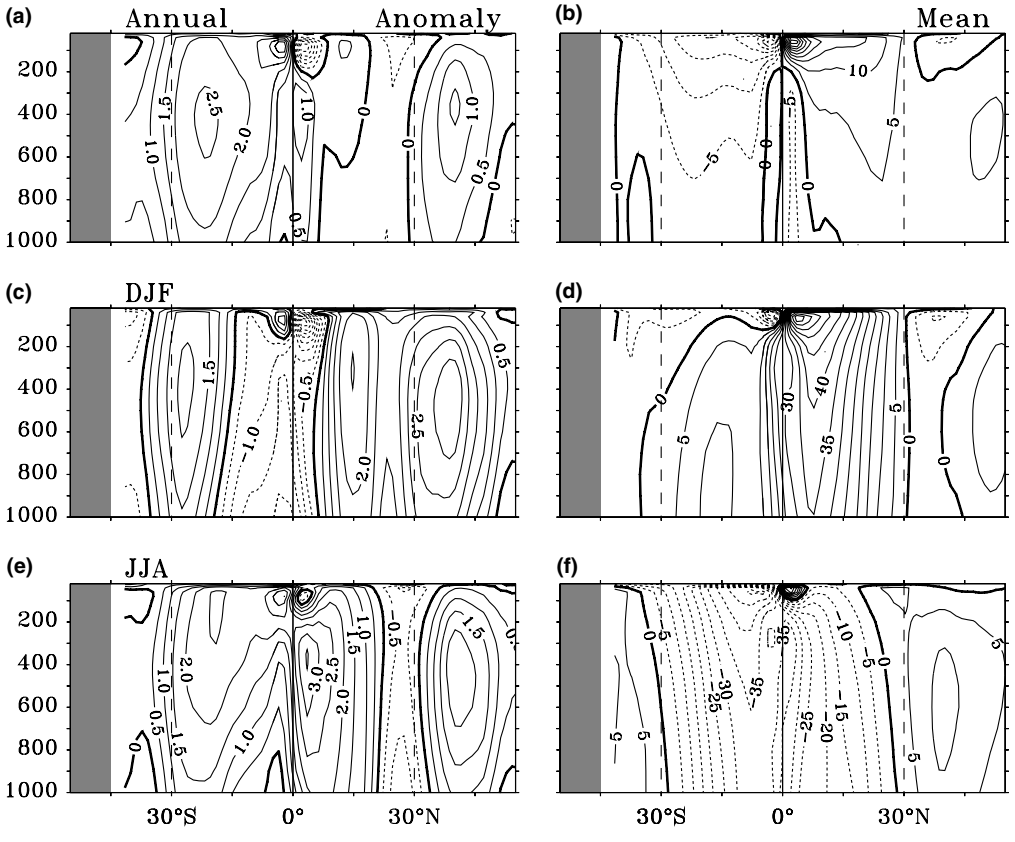


**Fig. 6** Meridional overturning streamfunction (STC) of the Pacific for (*right column*) the CTRL and (*left column*) the difference between ABOT and its control averaged in year 150–200, for **a**, **b** annual mean, **c**, **d** DJF and **e**, **f** JJA. Contour intervals are 0.5 Sv (1 Sv = $10^6$ $m^3$/s) in (**a**), (**c**) and (**e**), and 5 Sv in (**b**), (**d**) and (**f**)

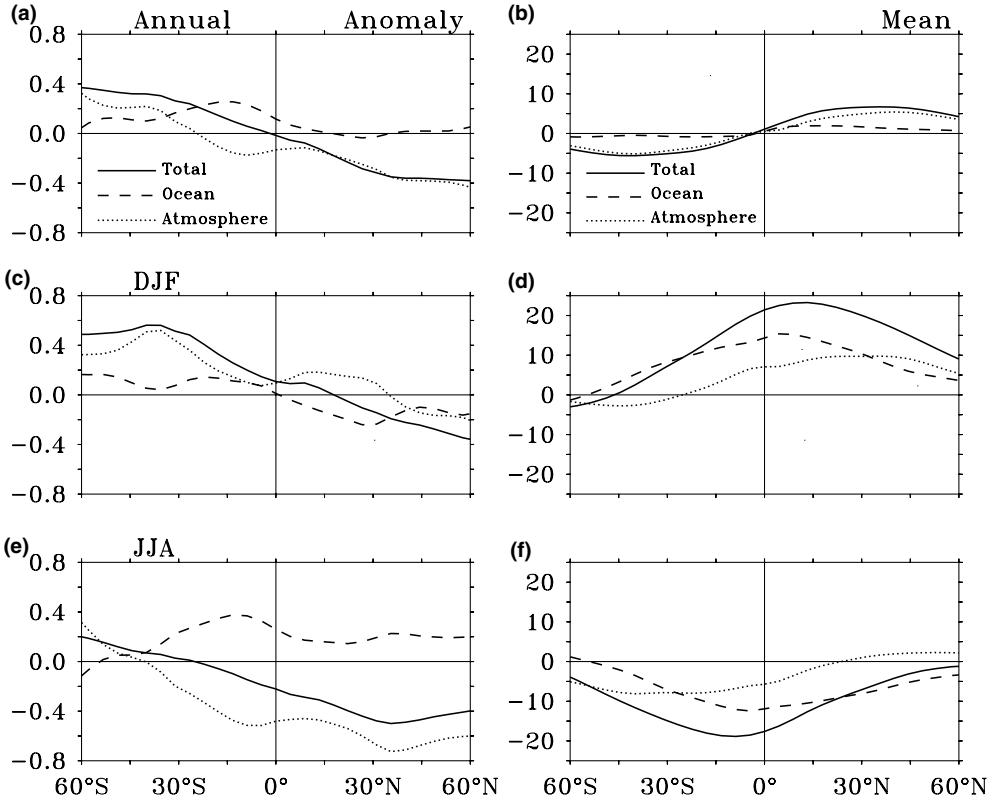


**Fig. 7** Meridional profiles of the northward heat transports for (*right column*) the CTRL and (*left column*) the difference between ABOT and its control averaged in year 150–200, for **a**, **b** annual mean, **c**, **d** DJF and **e**, **f** JJA. The solid lines represent the total heat transport by the atmosphere–ocean system, which is derived from the zonal and meridional integration of the net radiation flux (the net incoming solar radiation minus the net outgoing long wave radiation) at the top of the atmosphere. The *dashed lines* represent the total heat transport by global oceans, which is derived from the zonal and meridional integration of the net sea surface heat flux. The *dotted lines* represent the total heat transport by global atmosphere, which is indirectly obtained by subtracting the oceanic heat transport from the total heat transport at the top of the atmosphere because our climate model results do not have temporal precision high enough to resolve the atmospheric eddy activities which are thought to play dominant role in atmospheric heat transport. The unit in *y*-axis is $10^{15}$ W for all plots

overturning circulations. The annual mean heat transports by the atmosphere and ocean are poleward (Fig. 7b). The atmosphere plays a more important role in poleward heat transport than the ocean only in the annual mean sense. However, in the seasonal mean sense, the ocean transports more heat poleward than the atmosphere (Fig. 7d, f)

The extratropical warming in ABOT induces anomalous equatorward heat transports in both the atmosphere and ocean. In the annual mean sense (Fig. 7a), the oceans tend to bring anomalous heat from the southern oceans to the equator and further to the south of 15°N of the northern oceans (dashed line in Fig. 7a). This is in good agreement with the larger southern STC change in Fig. 6a. To balance the northward oceanic heat transport, the atmosphere brings anomalous heat from the NH to the north of 20°S of the SH (dotted line). The total anomalous heat transport by the atmosphere–ocean system is equatorward, which is nearly symmetric about the equator (solid line). In boreal winter (Fig. 7c), the total anomalous heat comes from the SH, in which the atmosphere transports the anomalous heat all the way to the 30°N of the NH, while the anomalous oceanic heat transport converges toward the equator. The latter is consistent with the symmetric change about the equator in the northern STC in Fig. 6c. The anomalous heat transports in boreal summer (Fig. 7e) are almost opposite to those in winter. The atmosphere brings anomalous heat from the NH to the SH while the ocean does the opposite.

Both the SH and NH are equivalently critical to the climate change in the tropics. Figure 7 shows that the oceans in the SH and the atmospheres in the NH play more important roles in modulating the tropical climate (Fig. 7a, e). The asymmetric changes in Hadley cells in ABOT result in asymmetric changes in the oceanic overturning circulations, even though the extratropical forcings are symmetric about the equator. The oceanic heat transport is mainly accomplished by mean flow, while the atmospheric heat transport is mainly accomplished by eddy activities. Therefore, the anomalous equatorward heat transport by the oceans comes mainly from the SH, while that by the atmospheres comes mainly from the NH because of more dramatic eddy activities there even though the larger change in Hadley cell occurs in the SH. However, because of huge differ-

ence of the thermal inertia between the atmosphere and ocean, the atmospheric adjustment occurs on monthly time scales, while the oceanic process occurs on interannual to decadal time scales. This implies that the NH is more important to the short-term climate change in the tropics, while the SH is more important to the secular change in the tropical climate.

### 3.4 Mechanisms

To understand the dynamic mechanism of the rapid tropical SST warming in the first few years in ABOT (Fig. 2a), a set of 12-member ensemble PC experiments are performed. Using the identical model configurations to ABOT, each experiment is restarted from different restart files of the control simulation of ABOT and integrated for 12 years. These ensemble experiments are composed into an ensemble mean for analysis. Monthly data is used here and the mean seasonal cycle has been removed because all anomalous quantities are derived as the difference of the PC experiments from their control runs, where they have the same seasonal cycle.

#### *3.4.1 Thermodynamics: surface heat budget*

After the onset of the extratropical warming, the global atmosphere responds very quickly, in months. Although the larger change in Hadley cell occurs in the SH, the anomalous atmospheric heat transport from the NH immediately warms up the tropical atmosphere (Fig. 8a, dashed black) in the first month. The tropical SST starts to increase about 2 months later (solid black), reaches the maximum at the end of the second year, and is then slightly reduced after that. There is about 2 months lead in atmosphere temperature to the SST during the first year. The warmer atmosphere emits more long-wave radiation that is absorbed by the sea surface, causing the SST rise. The subsurface temperature (solid grey) rises by merely 0.1°C in the first year, in sharp contrast to the 0.6°C increase in SST.

The dominant contribution to the tropical SST warming in the first few months, however, is due to the reduced latent heat flux to the atmosphere, instead of the increased net radiation flux absorbed by the sea surface. As mentioned before, one of the immediate consequences of the weakened Hadley cell is the weakening of the equatorial trade winds. The weakened trade winds result in less latent heat flux lost to the atmosphere (solid grey, Fig. 8b) by reducing surface evaporation, and eventually warm the SST. During this stage, the anomalous latent heat flux is a driving mechanism to the SST warming. It contributes nearly 80% of the total positive net heat flux (solid black, Fig. 8b) during the first 6 months. Less than 10% of the net heat flux is due to the increased net surface radiation (dashed grey). The remaining 10% contribution comes from the reduced sensible heat flux (dashed black) because of reduced trade wind and air-sea temperature difference.

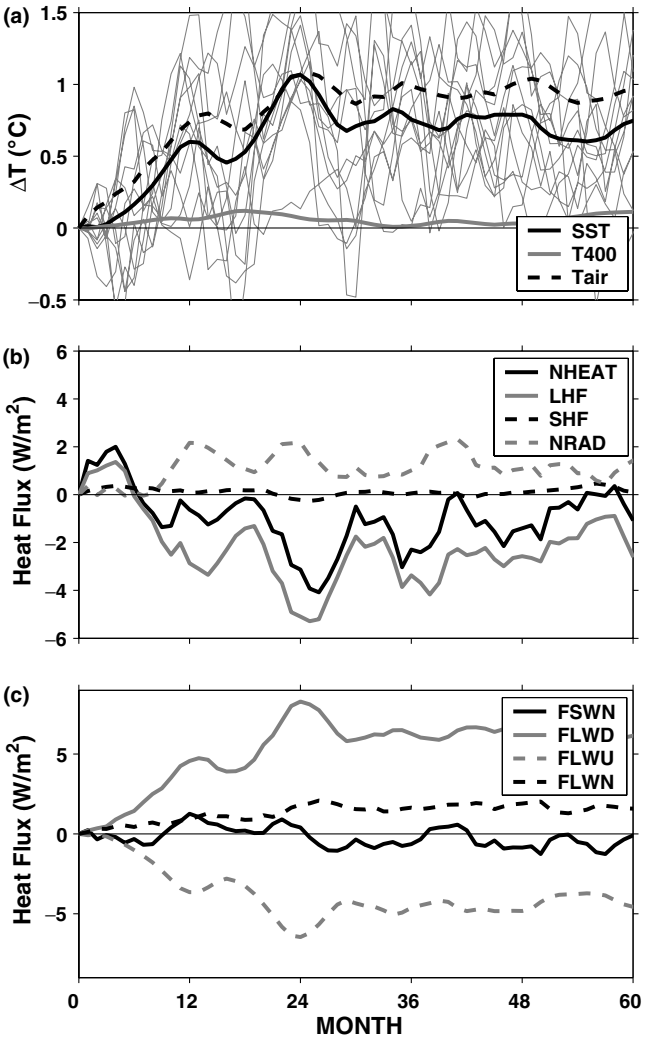


**Fig. 8** **a** Evolution of ensemble anomalous SST (*solid black*), subsurface temperature (40–400 m average) (*solid grey*) and vertical weight-averaged atmosphere temperature (*dashed black*) for the first 5 years in ABOT. The *thin solid grey lines* represent anomalous SST for each ensemble experiments. **b** Evolution of ensemble anomalous net heat flux (NHEAT) (*solid black*), latent heat flux (*LHF solid grey*), sensible heat flux (*SHF dashed black*) and net radiation flux (*NRAD dashed grey*). **c** Evolution of ensemble anomalous net short wave radiation (*FSWN*, *solid black*), downward long wave radiation (*FLWD solid grey*), outgoing long wave radiation (*FLWU dashed grey*) and net long wave radiation (*FLWN dashed black*). The net radiation flux (NRAD) is the sum of the FSWN and FLWN. In (**b**) and (**c**), all the curves are for the heat flux at the surface of the ocean, and positive value represents flux downward to the ocean. All the data are monthly data with seasonal cycle removed and averaged within 10°S−10°N of the Pacific

The increased net surface radiation is the result of increased downward long wave radiation due to the warmer atmosphere (Fig. 8c). The net surface radiation consists of the net short wave flux and net long wave flux at the surface. The net surface short wave flux (solid black) hardly changes because the cloud cover remains almost unchanged in ABOT (figure not shown), so that it does not contribute to the SST warming. The

increased net long wave radiation (dashed black) is mainly due to the increased incoming long wave radiation at the surface (solid grey). The outgoing long wave radiation depends on the SST, and usually acts as a damping factor to the SST warming (dashed grey).

The net surface heat flux becomes negative around 6 months after the onset of extratropical warming (solid black, Fig. 8b) and exerts a damping effect on the tropical SST warming thereafter. Although the atmosphere keeps emitting more long wave radiation to the ocean surface because of continuously increasing air temperature (dashed grey, Fig. 8b), the ocean loses more heat to the atmosphere because of increasing latent heat flux loss. During this stage, the warming SST, in turn, increases the surface evaporation that eventually overcomes the positive effect by the weakened trade wind. The latent heat flux loss is increased and acts as a damping effect on the SST, and reverses the role of the net surface heat flux in the SST warming. Therefore, the thermodynamic processes at the ocean–atmosphere interface are only partly responsible for the SST warming. The ocean dynamics must step in and play a crucial role in the persistent SST warming.

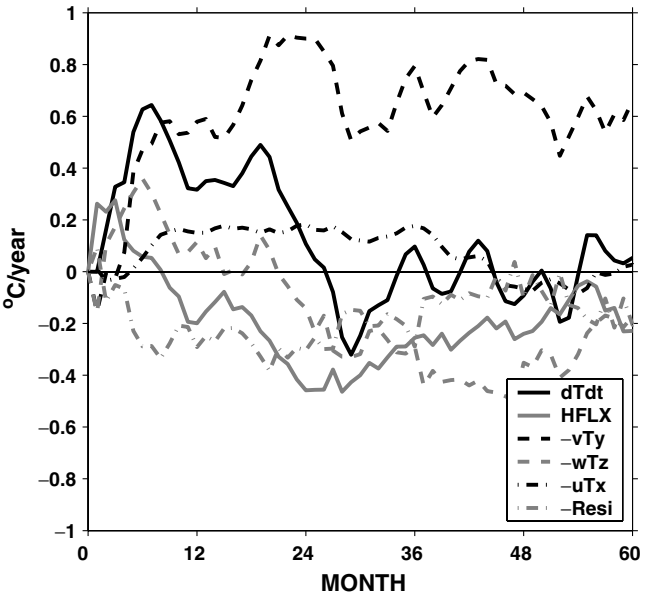


**Fig. 9** Evolution of the ensemble term balance of the surface box of equatorial Pacific (10°S–10°N, surface to 40 m) for the first 5 years in ABOT. The total temperature tendency ($\partial T/\partial t$), surface net heat flux (*HFLX*), meridional temperature advection ($-vT_y$), vertical temperature advection ($-wT_z$), zonal temperature advection ($-uT_x$) and residual term (Resi, vertical mixing and convection) are plotted as *solid black*, *solid grey*, *dashed black*, *dashed grey*, *dash-dotted black*, and *dash-dotted grey lines*, respectively. The horizontal mixing terms ($A_h\ T_{xx}$ and $A_h\ T_{yy}$) are negligible (not plotted here). Note that all terms are anomalous terms shown in Eq. (2)

### 3.4.2 Ocean dynamic feedback: term balance

To further understand the dynamic mechanism of the tropical SST warming, the term balance is analyzed within 10° of the equatorial Pacific (see Appendix). Two oceanic boxes are selected, in which the surface and subsurface boxes extend from surface to 40 m and from 40 to 400 m, respectively. Term balance analysis for the surface box shows that weakened meridional temperature advection $-(vT_y)'$ is the main reason for the tropical SST warming from the sixth month to the end of the second year (dashed black, Fig. 9). In fact, this term exceeds the net heat flux at the fourth month, and becomes the dominant driving term to maintain the positive temperature tendency $\partial T'/\partial t$ (solid black, Fig. 9) after the sixth month when the net heat flux becomes negative. The further decomposition of $-(vT_y)'$ shows that it is predominantly contributed by the weakened poleward Ekman transport $-v'T_y$ (solid grey, Fig. 10a), while the meridional temperature gradient change $-vT'_y$ (dashed black) and the nonlinear term $-v'T'_y$ (dashed grey) are negligible.

The vertical advection $-(wT_z)'$ (dashed grey, Fig. 9) also enhances the positive $\partial T'/\partial t$ during the first 2 years, because of weakened cold-water upwelling $-w'T_z$ (solid grey, Fig. 10b) in response to the weakened equatorial trade wind. However, $-(wT_z)'$ becomes negative due to the damping effect of mean upwelling $-wT'_z$ (dashed black, Fig. 10b). This occurs because SST increases rapidly while the subsurface temperature changes little, which in turn increases the vertical temperature gradient ($T'_z > 0$), resulting in negative $-wT'_z$ ($w > 0$) and eventually slowing down the SST warming. The zonal advection $-(uT_x)'$ (dash-dotted black, Fig. 9) also has a positive contribution to $\partial T'/\partial t$. The vertical diffusion and convection (dash-dotted grey, Fig. 9), however, always tend to retard the SST warming.

The different SST heat budget before and after the sixth month suggest a two stage SST rise in the first 2 years, both being caused by the atmospheric bridge teleconnection from the extratropics. The first stage occurs before the sixth month, in which the equatorial SST is warmed directly by the local atmospheric effect, mainly through the reduced surface latent heat flux. The second stage occurs afterwards, with the SST warming caused mainly by the reduced oceanic advective cooling, which is mainly caused by the reduction of the local equatorial cell (Fig. 6). This local oceanic effect can be viewed as the dynamic oceanic feedback to the reduced equatorial trade winds, which in turn is caused by the atmospheric teleconnection from the extratropics. Since the oceanic warming is comparable in these two stages (each about 0.3°C, Fig. 8a), the equatorial oceanic dynamic feedback is as important as the direct atmospheric effect in the warming of the equatorial SST.

### 3.4.3 Perturbation advection and mean advection

The slow equatorial temperature increase after the rapid initial warming in ABOT is comparable to the slow equatorial temperature increase in OT (Fig. 2a), both of

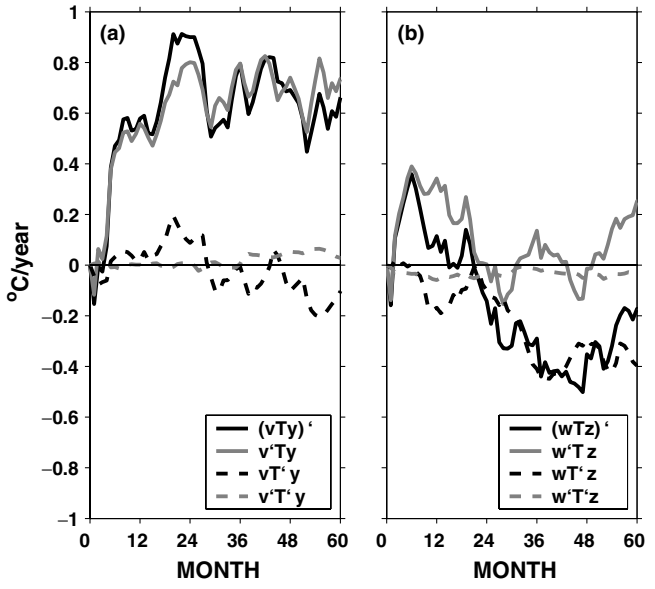


**Fig. 10** Decomposition of **a** the meridional temperature advection and **b** the vertical temperature advection in ABOT for the surface box of equatorial Pacific (10°S–10°N, surface to 40 m). The *solid black line* represent the total temperature advection changes ($-(vT_y)'$, $-(wT_z)'$) that have been shown in Fig. 9. The perturbation advection terms ($-v'T_y$, $-w'T_z$) and mean advection terms ($-vT'_y$, $-wT'_z$) are plotted as *solid grey line* and *dashed black line*, respectively. The nonlinear terms ($-v'T_y'$, $-w'T'_z$) are very small and plotted as *dashed grey line*

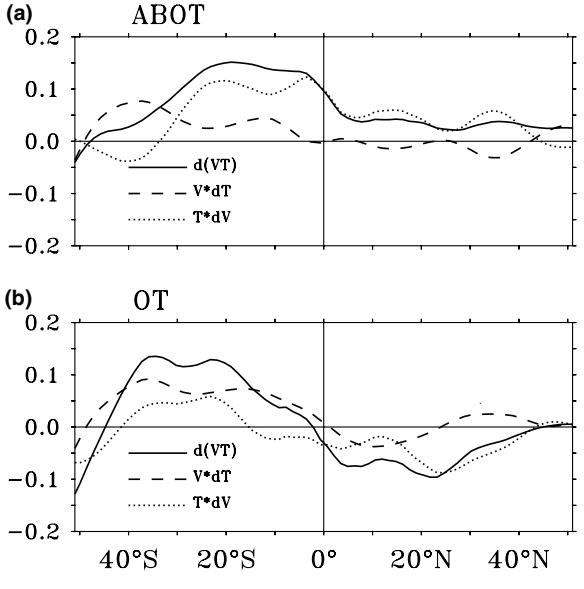


**Fig. 11** The Pacific anomalous heat transport for **a** ABOT and **b** OT averaged in year 150–200. The heat transport is calculated as vertical and zonal integration of $vT$. The total anomalous heat transport in (**a**) and (**b**) is $(vT)'$ (*solid line*). The decomposition of $(vT)'$ are $vT'$ (*dashed line*) and $v'T$ (*dotted line*), which represent the mean advection mechanism and the perturbation advection mechanism, respectively. The nonlinear term $v'T'$ is negligible and not plotted

which are due to the mechanism of the OT. Two oceanic mechanisms, both of which are related to the STCs, are responsible for the equatorial temperature change. Changes in the STCs' strength, referred to as the perturbation advection mechanism ($-v'T$), can cause the equatorial temperature change by varying the amount of meridional cold-water transport (Kleeman et al. 1999; Nonaka et al. 2002). Meanwhile, the extratropical temperature anomaly can also be transported equatorward by mean subduction flow (or mean STC) (Gu and Philander 1997; Zhang et al. 1998b) to affect equatorial temperature, which is called the mean advection mechanism ($-vT'$). Since the strength of the STCs depends only on wind forcing and not buoyancy forcing, these two mechanisms work simultaneously in ABOT, but only the mean advection mechanism works in OT. In ABOT, the strength of the STCs is reduced by over 10% (Fig. 6a), while the STCs in OT remain almost unchanged (figure not shown) because the atmospheric climatology is the same as in CTRL.

The decomposition of the anomalous oceanic heat transport ($-[vT]'$) confirms that in ABOT the weakened STCs ($-v'T$) contribute most of the anomalous equatorward heat transport (mainly through the SH) (dotted line, Fig. 11a) because less warm (cold) water flows out of (into) the tropics at the surface (depth), while the warm temperature anomaly ($-vT'$) subducted from the extratropics by the mean STCs (dashed line, Fig. 11a) only comprises a very small part of the equatorward heat transport. In contrast, the $-(vT)'$ in OT is mainly contributed by the $-vT'$ (dashed line, Fig. 11b), while the contribution from $-v'T$ is secondary (dotted line, Fig. 11b). In summary, although the equatorial thermocline change is of the same magnitude in ABOT and OT, the mechanisms are different: the perturbation advection mechanism is dominant in ABOT while the mean advection mechanism is more important in OT. Consistent with the mean advection mechanism in OT, the equatorward warm tongue in the SH is very clear in OT (Fig. 3d2), but not obvious in ABOT (Fig. 3b2).

### *3.4.4 Term balance in the final steady state*

The upper ocean temperature in the tropics nearly reaches equilibrium 100 years after the onset of the remote warming (Fig. 2). Term balance analysis of the final steady state is shown in Fig. 12. For better understanding of the term balance in ABOT and OT, the mean climatology of term balance is also plotted in Fig. 12a and 12b. Usually the equatorial ocean surface (Fig. 12a) receives heat from the solar radiation flux, which is partly transported to the extratropics by poleward Ekman flow ($v>0$, $T_y>0$, thus $-vT_y<0$, for the North of Equator) and partly damped by cold-water upwelling from the subsurface ($w>0$, $T_z>0$, thus $-wT_z<0$). The equatorial thermocline (Fig. 12b), however, is maintained by the equatorward heat transport from the extratropics (for the North of Equator, $v<0$, $T_y>0$, thus $-vT_y>0$) and damping effect of the cold-water upwelling ($-wT_z<0$) and vertical temperature mixing (Residual term, $T_{zz}<0$). Vertical mixing is very

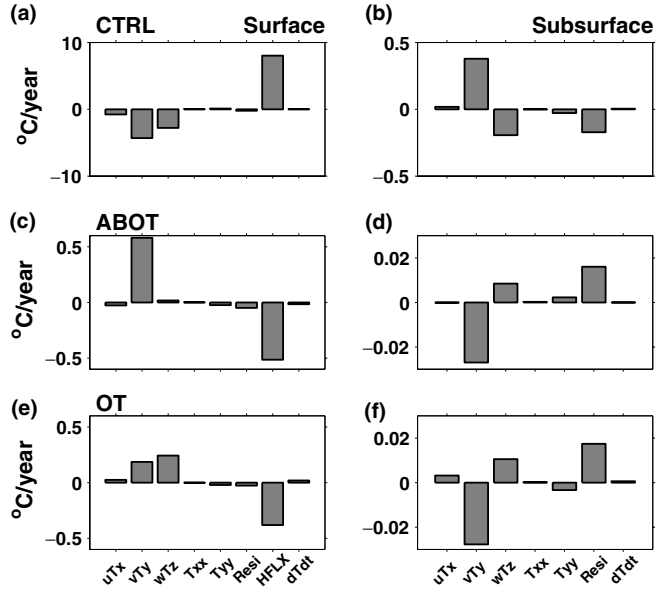


**Fig. 12** The term balance of (*left*) surface and (*right*) subsurface box of the equatorial Pacific (10°S–10°N) averaged in year 150–200. The total term balance for CTRL is plotted in **a** for surface and **b** for subsurface. The anomalous term balance is plotted in (**c**)–(**d**) for ABOT, and (**e**)–(**f**) for OT. From left to right, the terms are $-uT_x$, $-vT_y$, $-wT_z$, $T_{xx}$, $T_{yy}$, Residual term ($T_{zz}$ and vertical convection), net surface heat flux (HFLX, zero for subsurface) and $\partial T/\partial t$

important in the formation and maintenance of the equatorial thermocline.

Unlike the mean state, the increased SST in ABOT (Fig. 12c) is maintained by the balance between the warming effect from weakened poleward temperature advection ($-(vT_y)' > 0$) and cooling effect from the increased outgoing surface net heat flux; the increased subsurface temperature (Fig. 12d), however, is maintained by the balance between the warming effects from vertical temperature advection ($-(wT_z)' > 0$) and residual term (vertical mixing, $T'_{zz} > 0$), and the cooling effect from the meridional temperature advection ($-(vT_y)' < 0$). Notice that the meridional temperature advection plays an opposite role in the equatorial surface and subsurface temperature changes. Further decomposition of $-(vT_y)'$ and $-(wT_z)'$ shows that they are primarily caused by weakened STCs (For surface box, $v' < 0$, $T_y > 0$, thus $-v'T_y > 0$. For subsurface box, $v' > 0$, $T_y > 0$, thus $-v'T_y < 0$; $w' < 0$, $T_z > 0$, thus $-w'T_z > 0$), consistent with the perturbation advection mechanism.

The mechanism of SST increase in OT is quite different from that in ABOT as mentioned before. In OT, the equatorial SST is mainly warmed from below by the OT. Term balance analysis confirms that the positive anomalous vertical temperature advection ($-(wT_z)' > 0$) is the dominant term for the SST warming (Fig. 12e). Further, positive $-(wT_z)'$ results from anomalous warm-water upwelling from below ($w > 0$, $T'_z < 0$, thus $-wT'_z > 0$). Once the SST warms up, the increased outgoing latent heat flux tends to slow down the warming trend. Finally, the warming effect of $-wT_z'$ is balanced by the cooling effect of net heat flux. The term balance in subsurface temperature change in OT (Fig. 12f) is similar to that in ABOT (Fig. 12d); however, the negative $-(vT_y)'$ and positive $-(wT_z)'$ are the results of negative $-vT'_y$ ($v < 0$, $T'_y < 0$) and positive $-\mathrm{w}T'_z$ ($w > 0$, $T'_z < 0$), consistent with the mean advection mechanism.

## 4 Tropical impact on extratropical climate

The quantitative impact of the tropics on the extratropical climate remains uncertain, although the tropics has long been recognized as crucial for global climate through atmospheric teleconnections (Lau 1997; Alexander et al. 2002). The PC experiment T-ABOT reveals that the tropical impact on extratropical climate is as strong as the extratropical impact on tropical climate. Both the extratropical SST (Fig. 2a) and subsurface temperature (Fig. 2b) are warmed finally by about 1°C after the onset of the 2°C tropical warming, comparable with the tropical warming in ABOT.

In contrast to ABOT and OT, in which the equatorward ocean tunnel is important, the poleward ocean tunnel in T-ABOT seems to be ineffective. In other words, the tropical impact on the extratropical climate is predominantly accomplished by the atmospheric process. The weakness of the poleward ocean tunnel in T-ABOT is also supported by another sensitivity experiment (T-OT, not shown) in which the poleward atmospheric bridge is shut off similarly as in OT. The final SST in the extratropics changes little after 200 years. Physically, the poleward ocean tunnel mainly consists of the surface Ekman flow, which tends to generate near-surface temperature anomaly tongues moving toward the mid-latitude. These near-surface tongues, however, are easily damped by the strong negative air-sea feedback, as seen in T-ABOT at about 30–35° latitude (Fig. 3c2).

The atmospheric bridge in T-ABOT causes extratropical temperature changes in both the surface and subsurface. The Hadley cell in T-ABOT is strengthened by about 10% because of increased meridional SST gradient. This also results in an equatorward shift of the baroclinic eddy activity in the atmosphere that eventually reduces the cloud cover in the extratropics (Figure not shown), increasing shortwave radiation. The greater poleward heat transport by the atmosphere and increased shortwave radiation absorbed by the ocean overcome the evaporation cooling induced by the increased mid-latitude westerly winds due to enhanced Hadley cell, increasing the extratropical SST. The atmospheric impact on the extratropical SST is quickly mixed into the subsurface because of the deep oceanic mixed layer (Fig. 3a2) and stronger Ekman downwelling in the mid- and high- latitudes. This delays the surface warming, but hastens the subsurface warming. As a result, relative to the tropical temperature changes in ABOT, the initial warming in T-ABOT is slower on the surface (Fig. 2a) but faster in the subsurface (Fig. 2b). It

is worth noting that the final SST change has a local maximum at about 60°N/S in extratropics (Fig. 3c1), which may be related to the positive sea ice–albedo feedback mechanism (Curry et al. 1995). The warming in high latitudes reduces the extent of snow and sea ice, decreasing the surface albedo and increasing the radiation flux that is absorbed by the surface, resulting in a further rise in the local SST. This is different from the equatorial SST maximum in ABOT and OT, which is generated by warm anomaly upwelling of oceanic tunnel.

The STCs in T-ABOT are also enhanced in response to the stronger Hadley cell. This causes stronger Ekman downwelling in the extratropics as well as stronger Ekman upwelling in the tropics. Consequently, the extratropical thermocline can be easily disturbed by surface warming, while the tropical thermocline cannot be disturbed. This can be seen in Fig. 3c2, illustrating that the vertical temperature gradient is weak in extratropics but strong in tropics.

## 5 Relative impacts of the NH and SH on the tropics

The SH appears to contribute more than the NH to the equatorial secular climate change as suggested in Figs. 3, 4, 5 and 6. Here, four more PC experiments (N-ABOT, S-ABOT, N-OT and S-OT) are performed to explicitly quantify the contributions of SH and NH to the equator. Similar to ABOT, in N-ABOT, the 2°C SST anomaly is "seen" by both the atmosphere and ocean only in the global NH ($>30°$N), and the mean SST seasonal cycle of the CTRL is prescribed in the global SH ($>30°$S). In N-OT, only the ocean "sees" a 2°C SST warming and therefore, contributes to the southward subduction of extratropical SST anomaly. The configurations in S-ABOT and S-OT are opposite to those in N-ABOT and N-OT, respectively. The full coupling in these four experiments is still confined to the global tropics ($<|30°|$).

The SH (solid grey, Fig. 13a) contributes 30% more than the NH (solid black) to the equatorial SST as suggested by S-ABOT and N-ABOT (0.53 vs. 0.40), mainly through the atmospheric bridge because the SST warming in S-OT (dashed grey) and N-OT (dashed black) are almost the same (0.14 vs. 0.13) (Fig. 13a). The equatorial subsurface temperature change in S-ABOT is 50% more than that in N-ABOT (0.64 vs. 0.43). However, through only the OT, the subsurface temperature change in S-OT is about 70% more than that in N-OT (0.55 vs. 0.32) (Fig. 13b). The total equatorial temperature change in S-ABOT and N-ABOT is 0.93°C (1.07°C) for surface (subsurface), and the total temperature change in S-OT and N-OT is 0.27°C (0.87°C) for surface (subsurface), all of which are in good agreement with the 0.87°C (1.03°C) in ABOT and the 0.26°C (0.87°C) in OT (Fig. 2).

The larger contribution to the equatorial thermocline from the SH results from the larger SH STC change in S-ABOT or stronger equatorward subduction of anomalous signal from the SH in S-OT. This can be clearly seen in Fig. 14. The equatorward warm tongue in S-OT (Fig. 14e2) is stronger than that in N-OT (Fig. 14f2), illustrating that more warm anomaly is subducted to the equator by mean flow from the SH, which is also consistent with mean advection mechanism. However, this

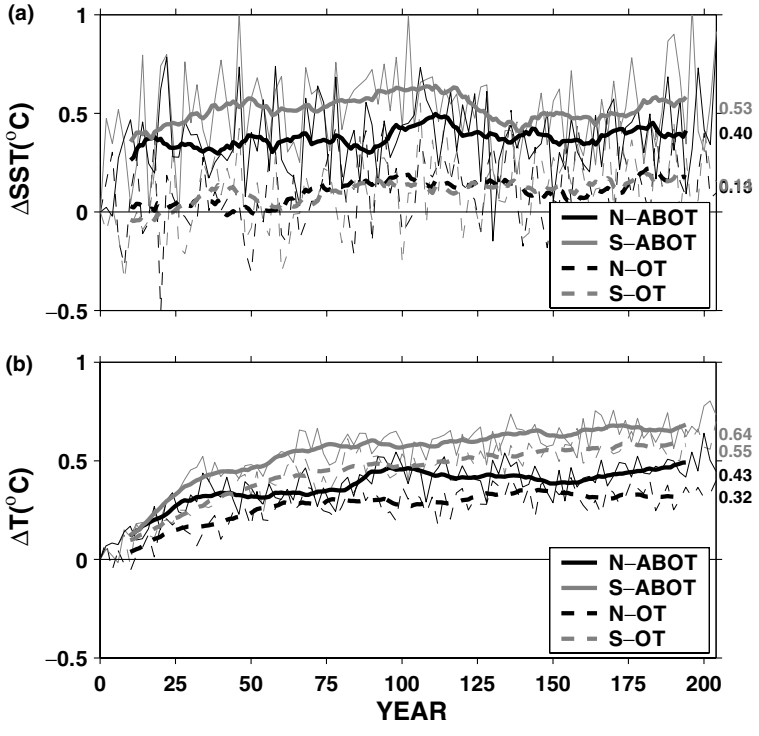


**Fig. 13** Same as Fig. 2, but for PC experiments N-ABOT (*solid black*), S-ABOT (*solid grey*), N-OT (*dashed black*) and S-OT (*dashed grey*)

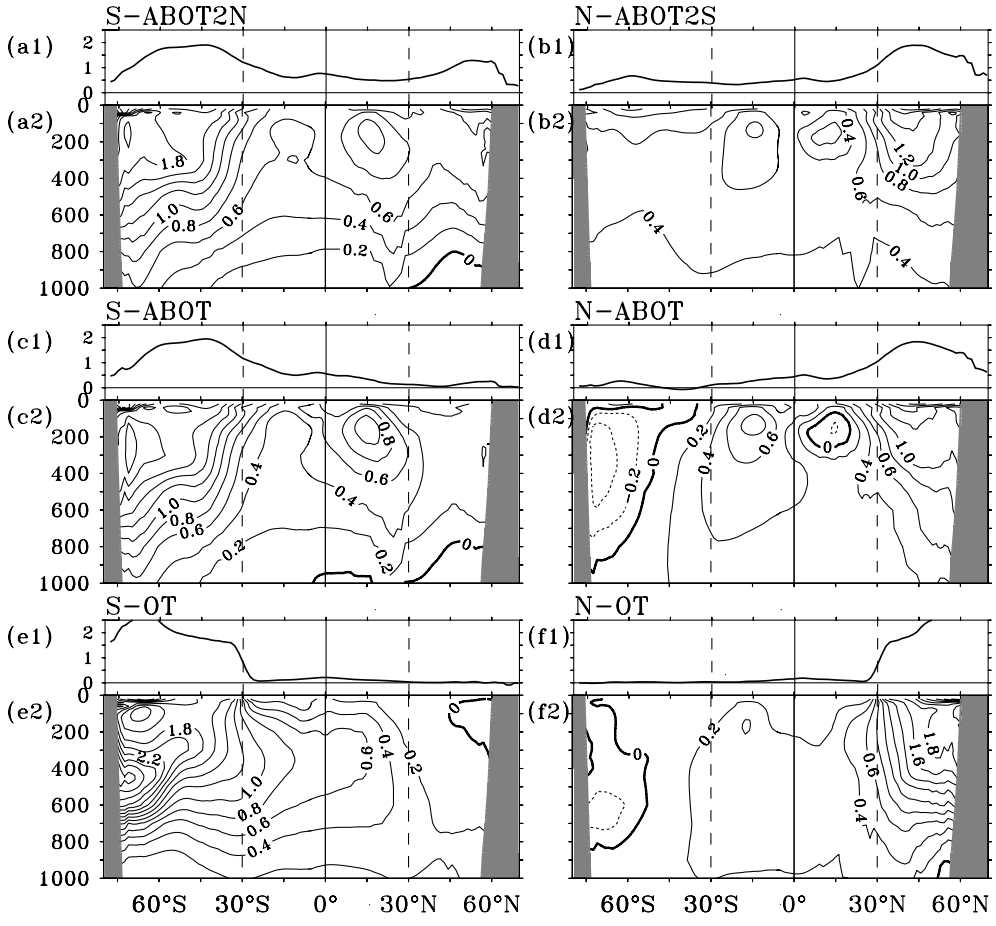


**Fig. 14** Same as Fig. 3, but for PC experiments **a** S-ABOT2N, **b** N-ABOT2S, **c** S-ABOT, **d** N-ABOT, **e** S-OT and **f** N-OT

warm tongue is less obvious in both S-ABOT and N-ABOT. The temperature change in both the tropics and extratropics in S-ABOT (Fig. 14c2) is larger than those in N-ABOT (Fig. 14d2), suggesting that it is mainly the STC change, or more precisely, the SH STC change that results in equatorial subsurface temperature change.

The SH SST warming can further induce remarkable remote climate change in the NH and vice versa. This is explicitly revealed by another two PC experiments (N-ABOT2S and S-ABOT2N). N-ABOT2S (S-ABOT2N) is similar to N-ABOT (S-ABOT) except that the fully coupled region is extended to the whole SH (NH), so that the prescribed 2°C SST warming in the NH (SH) can further disturb the SH (NH) climate. After 200 years evolution, the final NH SST change in response to a 2°C SH SST forcing is about 0.8°C (dashed grey, Fig. 15). In contrast, the final SH SST change in response to a 2°C NH SST forcing is only 0.5°C (dashed black), nearly 60% smaller than the NH SST change. This suggests that the SH plays more important role in the global climate change.

The remote SST change in the NH (SH) in S-ABOT2N (N-ABOT2S) appears to be enhanced by positive sea ice–albedo feedback, generating a local maximum around 60°N (S) (Fig. 14a1, b1). This also might be the reason that the final remote SST change in the

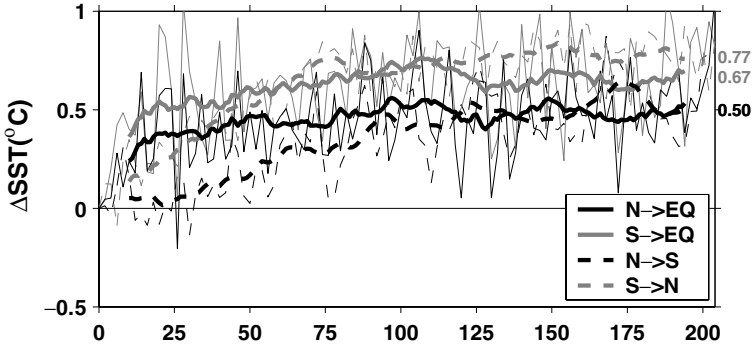


**Fig. 15** Same as Fig. 2a, but for PC experiments N-ABOT2S and S-ABOT2N. The tropical temperature changes are averaged globally from 10°S to 10°N for both experiments (*solid black* for N-ABOT2S, *solid grey* for S-ABOT2N). The remote SST changes in the NH (*dashed black*) and the SH (*dashed grey*) for S-ABOT2N and N-ABOT2S are averaged globally from 30°N to 60°N and from 30°S to 60°S

NH (SH) even exceeds the tropical SST changes. In S-ABOT2N and N-ABOT2S, the initial tropical SST warmings (solid grey and solid black, Fig. 15) are faster and stronger than the remote SST changes in the NH and SH (dashed grey and dashed black), but the former are gradually surpassed by the latter after several decades. This is particularly clear in S-ABOT2N, in which the final tropical SST warming (solid grey, Fig. 15) is about 0.7°C, more than 10% smaller than the remote NH SST change (dashed grey).

It is worth noting that the tropical SST changes in N-ABOT2S and S-ABOT2N (0.5°C and 0.67°C) are about 20–25% larger than those in N-ABOT and S-ABOT (0.4°C and 0.53°C). This may result from the feedback processes between the tropics and the NH (SH) extratropics in S-ABOT2N (N-ABOT2S). Because full coupling is allowed in both the tropics and the NH (SH) in S-ABOT2N (N-ABOT2S), the tropical SST warming strengthens the Hadley cell in the NH (SH) and warms the NH (SH) SST, which in turn reduces the meridional SST gradient and weakens the NH (SH) Hadley cell, causing an additional tropical SST rise. This feedback process also results in the ocean approaching the quasi-equilibrium at a slower pace (Fig. 15).

## 6 Conclusions and discussions

Tropical–extratropical climate interaction is studied in a fully coupled climate model. Model results show that the extratropical impact on tropical SST could be as strong as the tropical impact on extratropical SST, with the remote SST response being about half the magnitude of the imposed change in SST in the forcing region. The extratropical impact on tropical SST by the atmospheric bridge accounts for 70% of the change while the oceanic tunnel accounts for the remaining 30%; the extratropical control on the tropical subsurface temperature is contributed dominantly by the oceanic tunnel. This is in contrast to the tropical influences on the extratropical surface and subsurface temperature, both of which are accomplished by the atmospheric bridge.

The mechanism of tropical–extratropical climate interaction is carefully investigated. Different from the discussion in LY03, the effect of atmospheric bridge in ABOT is accomplished not only by the atmospheric effect on equatorial SST through the surface heat flux (especially the latent heat flux), but also by the equatorial oceanic dynamic feedback through the surface Ekman flow and upwelling. Therefore, about only half of the 70% effect of equatorial warming through the atmospheric bridge is due to the pure atmospheric effect, with the other half as the positive dynamic oceanic feedback on the equator. This latter effect won't exist in a model without dynamic ocean, such as a coupled atmosphere model with a slab mixed layer ocean. The slow equatorial SST and subsurface temperature changes result from both the change in STCs' strength and the equatorward subduction of anomalous signal (Only the latter was discussed in LY03). This effect alone is about 30% contribution to the equatorial SST warming as implied in the OT experiment. However, considering the important effect of equatorial dynamic feedback, ocean dynamics is more important than implied by the 30% effect of the oceanic tunnel alone.

The relative contributions of the two hemispheres to the equator are further investigated in this paper. It is explicitly shown that the dominant influence on the secular global climate comes from the SH. This is justified because the sea surface area in the SH is about 37% greater than in the NH. The SH and NH would weight equally in the global climate if they had the same sea surface area. The larger contribution of the SH is consistent with recent glacial climate simulations (Liu et al. 2002b) and the sensitivity experiments by an ocean general circulation model (Yang and Liu 2004), as well as observations (Johnson and McPhaden 1999). This stronger southern contribution may also shed light on paleoclimate records which show that the tropical temperature evolves synchronously with the Antarctic air temperature and atmospheric $CO_2$, but leads the NH continental ice volume (Lea et al. 2000).

More diagnoses are needed for the heating and transfer processes of the atmosphere. Since our model outputs from all experiments are monthly data, we are unable to directly calculate the meridional heat transport by atmospheric eddy activities. Instead, the atmospheric heat transport is indirectly estimated as the difference of the total heat transport of the air-sea system and the oceanic heat transport. The eddy activities play a dominant role in the meridional heat transport of the midlatitude atmosphere. However, we fail to explicitly distinguish atmosphere heat transport due to the eddy activities from that by mean Hadley cells because of the monthly data. We are going to run experiment ABOT for several more years and save the outputs as daily data so that we can diagnose the atmospheric processes for further details.

This work provides a quantitative estimate of the extratropical–tropical climate interaction, and a framework to quantify the roles of atmospheric and oceanic processes in the extratropical–tropical interactions in fully coupled models as well. All the results obtained here are appropriate for our model but also might be model-dependent. However, we expect that the mechanisms examined in our model and the understanding of climate interaction here would be helpful to understand reality. The major conclusions here have important implications for the study of global climate changes. For example, climate changes in the tropics should consider as the response not only to feedbacks within the tropics (e.g., Ramanathan and Collins 1991), but also to the climate change in the extratropics and the associated extratropical–tropical interactions. This work also provides clues to quantify the roles of earth system components in highly complicated models.

This paper is also relevant to the problem of mechanisms of climate adjustment to external forcing. The prescribed 2°C SST forcing in our sensitivity experiments is well beyond the range of intrinsic coupled variability, but is within the limit of the temperature sensitivity of 1.5–4.5°C for a doubling of $CO_2$ determined from paleoclimatic data (Lea 2004) and coupled models (Kerr 2004). The strong forcing in our experiments is necessary to generate significant change in the remote region. The idealized warming pattern in this work is different from the "real" greenhouse gas forcing scenario. However, this pattern as well as its global consequences could be one manifestation of a broad spectrum of possibilities, and thus, the study here could enhance our understanding of reality.

**Acknowledgements** This work is supported by NOAA, NASA, DOE and the NSF of China (no. 40306002). The authors thank Drs. R. Gallimore and L. Wu for help with the partial coupling program, and Ms. D. Lee for providing the term balance analysis package. The authors benefited from discussions with Drs. S. Vavrus, Q. Zhang, as well as the invaluable comments from Editor, Prof. E. K. Schneider and two anonymous reviewers.

## 7 Appendix

The term balance is analyzed within 10° of the equator in the Pacific. Two oceanic boxes are selected, in which the surface and subsurface boxes extend from surface to 40 m and 40 to 400 m, respectively. The terms in the temperature equation are:

$$\frac{\partial T}{\partial t} \sim -uT_x - vT_y - wT_z + A_h T_{xx} + A_h T_{yy} + \mathrm{HFLX} + \mathrm{Residual}. \quad (1)$$

Here, $\partial T/\partial t$ is the local temperature tendency; $-uT_x$, $-vT_y$ and $-wT_z$ are the zonal, meridional and vertical temperature advection, respectively; $A_h\ T_{xx}$, $A_h\ T_{yy}$ are the horizontal diffusion terms with the constant diffusion coefficient $A_h$ (4,000 $m^2$ /s); and heat flux *HFLX* is the surface net heat flux forcing (it is zero for the subsurface box). The residual term includes the vertical diffusion and convection. It is obtained by subtracting the other terms from $\partial T/\partial t$ since it cannot be explicitly calculated. Monthly data is used here. The changes of all terms used here are derived as the differences of the terms from ensemble PC experiments and their control. These anomalous terms are

$$\frac{\partial T'}{\partial t} \sim -(uT_x)' - (vT_y)' - (wT_z') + A_h T'_{xx} + A_h T'_{yy} + (\mathrm{HFLX})' + (\mathrm{Residual})', \quad (2)$$

where, $\partial\ T'/\partial\ t = (\partial T/\partial t)_{PC} - (\partial T/\partial t)_{\mathrm{CTRL}}$ and all other terms are similarly obtained. The temperature advection terms can be further decomposed as

$$-(uT_x)' = -u'T_x - uT'_x - u'T'_x, \quad (3)$$

$$-(vT_y)' = -v'T_y - vT'_y - v'T'_y, \quad (4)$$

$$-(wT_z)' = -w'T_z - wT'_z - w'T'_z. \quad (5)$$

Thus, the temperature advection change results from the changes of mean current ($-u'T_x$, $-v'T_y$, $-w'T_z$) and mean temperature gradient ($-u\overline{T}'_x$, $-v\overline{T}'_y$, $-w\overline{T}'_z$) as well as their nonlinear interactions ($-u'\overline{T}'_x$, $-v'\overline{T}'_y$, $-w'\overline{T}'_z$). The temperature gradient is positive poleward and upward.

## References

Alexander MA, Blade I, Newman M, Lanzante JR, Lau NC, Scott JD (2002) The atmospheric bridge: the influence of ENSO teleconnections on air-sea interaction over the global oceans. J Climate 15:2205–2231

Barlow M, Nigam S, Berbery EH (2001) ENSO, Pacific decadal variability, and US summertime precipitation, drought, and streamflow. J Climate 14:2105–2128

Barnett TD, Pierce W, Latif M, Dommenget D, Saravana R (1999) Interdecadal interactions between the tropics and the midlatitudes in the Pacific basin. Geophys Res Lett 26:615–618

Cane MA, Clement AC, Kaplan A, Kushnir Y, Pozdnyakov D, Seager R, Zebiak SE, Murtugudde R (1997) Twentieth-Century sea surface temperature trends. Science 275:957–960

Clement AC, Seager R, Cane MA, Zebiak SE (1996) An ocean dynamic thermostat. J Climate 9:2190–2196

Curry JA, Schramm JL, Ebert EE (1995) Sea ice–albedo climate feedback mechanism. J Climate 8:240–247

Enfield DB, Mayer DA (1997) Tropical Atlantic sea surface temperature variability and its relation to El Nino-Southern Oscillation. J Geophys Res 102:929–945

Gu D, Philander SGH (1997) Interdecadal climate fluctuations that depend on exchanges between the tropics and extratropics. Science 275:805–807

Hoerling M, Kumar A (2003) The perfect ocean for drought. Science 299:691–694

Hoerling MP, Hurrell JW, Xu T (2001) Tropical origins for recent North Atlantic climate change. Science 292:90–92

Jacob (1997) Low frequency variability in a simulated atmosphere ocean system. PhD Thesis, University of Wisconsin, p 155

Johnson GC, McPhaden MJ (1999) Interior pycnocline flow from the subtropical to equatorial Pacific Ocean. J Phys Oceanogr 29:3073–3089

Kerr RA (2004) Three degrees of consensus. Science 305:932–934

Kleeman R, McCreary JP, Klinger BA (1999) A mechanism for generating ENSO decadal variability. Geophys Res Lett 26:1743–1746

Lau NC (1997) Interactions between global SST anomalies and the midlatitude atmospheric circulation. Bull Am Meteor Soc 78:21–33

Lea DW (2004) The 100,000-year cycle in tropical SST, greenhouse forcing, and climate sensitivity. J Climate 17:2170–2179

Lea DW, Pak DK, Spero HJ (2000) Climate impact of late quaternary equatorial Pacific sea surface temperature variations. Science 289:1719–1724

Liu Z (1998) The role of ocean in the transient response of tropical climatology to global warming: the west–east SST contrast. J Climate 11:864–875

Liu Z, Wu L (2000) Tropical Atlantic oscillation in a coupled GCM. Atmos Sci Lett 1:26–36

Liu Z, Yang H (2003) Extratropical control of tropical climate, the atmospheric bridge and OT. Geophys Res Lett 30(5). doi: 10.1029/2002GL016492

Liu Z, Philander SDH, Pacanowski R (1994) A GCM study of tropical -subtropical upper ocean mass exchange. J Phys Oceanogr 24:2606–2623

Liu Z, Kutzbach J, Wu L (2000) Modeling climate shift of El Nino variability in the Holocene. Geophys Res Lett 27:2265–2268

Liu Z, Wu L, Gallimore R, Jacob R (2002a) Search for the origins of Pacific decadal climate variability. Geophys Res Lett 29(10):doi: 10.1029/2001GL013735

Liu Z, Shin S, Otto-Bliesner B, Kutzbach J, Brady E, Lee DE (2002b) Tropical cooling at the last glacial maximum and extratropical ocean ventilation. Geophys Res Lett 29(10). doi:10.1029/2001GL013938

Lu P, McCreary J, Klinger BA (1998) Meridional circulation cells and the source waters of the Pacific equatorial undercurrent. J Phys Oceanogr 28:62–84

Lu J, Greatbatch RJ, Peterson KA (2004) Trend in northern hemisphere winter atmospheric circulation during the last half of the 20th century. J Climate 17:3745–3760

McCreary J, Lu P (1994) On the interaction between the subtropical and the equatorial oceans: the subtropical cell. J Phys Oceanogr 24:466–497

McPhaden MJ, Zhang DX (2002) Slowdown of the meridional overturning circulation in the upper Pacific Ocean. Nature 415:603–608

Meehl GA, Washington WM (1996) El Niño-like climate change in a model with increased atmospheric $CO_2$ concentrations. Nature 382:56–60

Nonaka M, Xie SP, McCreary JP (2002) Decadal variations in the subtropical cells and equatorial Pacific SST. Geophys Res Lett 29(7). doi: 10.1029/2001GL013717

Pierce DW, Barnett TP, Latif M (2000) Connections between the Pacific Ocean Tropics and midlatitudes on decadal timescales. J Climate 13:1173–1194

Ramanathan V, Collins W (1991) Thermodynamic regulation of ocean warming by cirrus clouds deduced from observations of the 1987 El Nina. Nature 351:27–32

Rodgers K, Cane MA, Naik N, Schrag D (1999) The role of the Indonesian throughflow in equatorial Pacific thermocline ventilation. J Geophys Res 104:20551–20570

Schneider EK, Lindzen RS, Kirtman BP (1997) A tropical influence on global climate. J Atmos Sci 54:1349–1358

Seager R, Murtugudde R (1997) Ocean dynamics, thermocline adjustment and regulation of tropical SST. J Climate 10:521–534

Timmermann A, Latif M, Bacher A, Oberhuber J, Roeckner E (1999) Increased El Niño frequency in a climate model forced by future greenhouse warming. Nature 398:694–696

Wang C (2002) Atmospheric circulation cells associated with the El Nino-Southern oscillation. J Climate 15:399–419

Wu L, Liu Z, Gallimore R, Jacob R, Lee D, Zhong Y (2003) Pacific Decadal variability: the Tropical Pacific mode and the North Pacific mode. J Climate 16:1101–1120

Yang H, Liu Z (2004) Influence of extratropical thermal and wind forcings on equatorial thermocline in an ocean GCM. J Phys Oceanogr 34:174–187

Yu L, Rienecker MM (1999) Mechanisms for the Indian Ocean warming during 1997–1998 El Nino. Geophys Res Lett 26:735–738

Zhang Y, Wallace JM (1996) Is climate variability over the North Pacific a linear response to ENSO? J Climate 11:1468–1478

Zhang X, Sheng J, Shabbar A (1998a) Modes of interannual and interdecadal variability of Pacific SST. J Climate 11:2556–2569

Zhang RH, Rothstein LM, Busalacchi AJ (1998b) Origin of warming and El Nino change on decadal scales in the tropical Pacific Ocean. Nature 391:879–883